Supplementary Materials for

MAVS, cGAS, and endogenous retroviruses in T-independent B cell responses

Ming Zeng[1], Zeping Hu[2]^, Xiaolei Shi[2]^, Xiaohong Li[1]^, Xiaoming Zhan[1]^, Xiao-Dong Li[1,4], Jianhui Wang[1,4], Jin Huk Choi[1], Kuan-wen Wang[1], Tiana Purrington[1], Miao Tang[1], Maggy Fina[1], Ralph J. DeBerardinis[2], Eva Marie Y. Moresco[1], Gabriel Pedersen[3], Gerald M. McInerney[3], Gunilla B. Karlsson Hedestam[3], Zhijian J. Chen[1,4], Bruce Beutler[1]*

correspondence to: Bruce.Beutler@UTSouthwestern.edu

This PDF file includes:

Materials and Methods

Mice

C57BL/6J, *Rag2*$^{-/-}$, *Btk*$^{xid/Y}$, CBA/CaJ (controls for *Btk*$^{xid/Y}$), and *Igh*^{tm2Cgn} (*Igh*$^{B1-8}$) transgenic mice were purchased from The Jackson Laboratory. *Mavs*$^{-/-}$ *(23)*, *Sting*$^{gt/gt}$ (*Tmem173*$^{gt/gt}$) *(24)*, *cGas*$^{-/-}$ (*Mb21d1*$^{-/-}$) *(14)*, *Myd88*$^{-/-}$ *(25)*, and *Tlr3*$^{-/-}$ mice (*Tlr3*$^{tm1Flv/tm1Flv}$) *(26)* have been previously described. *Unc93b1*$^{3d/3d}$, *Tlr7*$^{rsq1/rsq1}$, *Tlr9*$^{CpG3/CpG3}$, *Tlr4*$^{lps3/lps3}$, *Tlr2*$^{languid/languid}$, *Cd36*$^{obl/obl}$, *Ticam1*$^{Lps2/Lps2}$, *Irak4*$^{otiose/otiose}$, *Nlrp3*$^{Park2/Park2}$, *Ikbkg*$^{panr2/Y}$, *Ifnar1*$^{macro-1/macro-1}$, and *Stat1*$^{dom/dom}$ strains were generated by *N*-ethyl-*N*-nitrosourea mutagenesis and are described at http://mutagenetix.utsouthwestern.edu; they are available from the Mutant Mouse Regional Resource Center. *Sting*$^{gt/gt}$*;Mavs*$^{-/-}$ mice were generated by intercrossing *Sting*$^{gt/gt}$ and *Mavs*$^{-/-}$ mice. *Ticam1*$^{Lps2/Lps2}$*;Irak4*$^{otiose/otiose}$ mice were generated by intercrossing *Ticam1*$^{Lps2/Lps2}$ and *Irak4*$^{otiose/otiose}$ mice. Mice were maintained at the University of Texas Southwestern Medical Center and studies were performed in accordance institutionally approved protocols.

For adoptive transfer, splenic B cells and peritoneal B cells were isolated using the Pan B cell Isolation Kit (Miltenyi Biotec). 2.5×10^7 splenic B cells were injected i.v. and 1.5×10^6 peritoneal cavity B cells were injected i.p. into *Rag2*$^{-/-}$ mice.

Immunizations

9-10 week old mice were immunized with rSFV-βGal (2×10^6 IU) on day 0 and NP_{49}-AECM-Ficoll (50 μg; Biosearch Technologies) on day 10 i.p. as previously described *(27)*. Blood was collected on day 14.5 after immunization with rSFV-βGal for ELISA analysis or immune cell analysis by flow cytometry. Mice were immunized with 50 μg NP-LPS (Biosearch Technologies) and blood was collected on day 4.5 post-immunization for ELISA analysis. Mice were immunized with 20 μg Pneumovax 23 (Merck) *(28)* or 20 μg *S. pneumoniae* PS1 and PS3 (ATCC) dissolved in 100 μl 0.9% saline (Teknova) and blood was collected on day 4.5 or 5.5 post-immunization for ELISA analysis.

For determination of the effect of cGAMP on NP-specific IgM production *in vivo*, C57BL/6J and cGAS-deficient mice were injected i.p. with 50 μg NP_{49}-AECM-Ficoll plus 20 μg 2'3'-cGAMP (Invivogen) in 200 μl 0.9% saline or with 0.9% saline alone (as the vehicle control). Blood was collected at day 5 post-immunization for ELISA analysis.

For determination of the effect of RT inhibitors on cytoplasmic ERV DNA levels or NP-specific IgM production *in vivo*, mice were injected i.p. with AZT (10 mg/ml; Selleckchem) and NVP (0.5 mg/ml; Selleckchem) once per day for 3 days before immunization. The same dosage of the RT inhibitors was continued following NP-Ficoll immunization until blood or splenic B cells were collected for analysis on day 4 post-immunization.

Blood was collected in Minicollect Tubes (Mercedes Medical), centrifuged at 700*g* to separate serum, and red blood cells remaining in the serum lysed (eBioscience) before immune cell staining and flow cytometric analysis. For ELISA analysis of antibody responses, Nunc MaxiSorp® flat-bottom 96-well microplates (Thermo Scientific) were coated with 2 μg/ml βGal (Roche), 5 μg/ml NP_8-BSA (Biosearch Technologies), 5 μg/ml

pneumococcal polysaccharides type 1 and 3 (ATCC) or 10 μg Pneumovax23 (Merck) at 4 °C overnight. Plates were washed four times with washing buffer (0.1% *v/v* Tween-20 in PBS) using a BioTeck microplate washer then blocked with ELISA Blocker Blocking Buffer (Thermo Scientific) for 1 hour at room temperature. Serum samples were serially diluted in ELISA Blocker Blocking Buffer (Thermo Scientific) and then the 1:50 and 1:150 dilutions were added to the prepared ELISA plates. After 1 hour incubation, plates were washed eight times with washing buffer and then incubated with HRP-conjugated goat anti-mouse IgM or IgG for 1 hour at room temperature. Plates were washed eight times with washing buffer then developed with SureBlue TMB Microwell Peroxidase Substrate and TMB Stop Solution (KPL). Absorbance was measured at 450 nm on a Beckman Coulter DTX880 Microplate Reader. Basal levels of anti-βGal IgG and anti-NP IgM were determined using pre-immune serum. The antigen-specific IgG and IgM were determined as the O.D. value post-immunization minus the O.D. value before immunization for each individual mouse. All ELISA data shown represent the 1:150 serum dilution.

Flow cytometry

Blood cells, splenocytes, or peritoneal cells were isolated and incubated for 1 hour at 4°C with mAb to CD16 and CD32 (BD Pharmingen) followed by consecutive labeling, each for 1 hour at 4°C, with one or more fluorochrome-conjugated mAb recognizing the following murine cell surface markers: CD25 (Biolegend); CD3, CD4, CD5, CD8α, CD11c, CD19, CD21/35, CD23, CD43, NK1.1, F4/80, Ly6G, GL7 and B220 (BD Pharmingen); CD80 and CD86 (eBioscience); and MHCII (eBioscience). The cells were then stained with Ghost Dye™ Violet 510 or Ghost Dye™ Violet 450 (Tonbo Bioscience) to identify live cells according to the manufacturer's instructions. Human B cells were stained in the same manner using HLA-DR, CD69 (Biolegend); and CD80 antibodies (BioLegend). NP-PE (Biosearch Technologies) was used to label NP-specific B cells. For detection of cytokines, antibodies against TNFα, IL-6, IL-12 (BD Pharmingen), and IFNβ (PBL Interferon Source) were used. For the detection of endogenous MLV-specific Env glycoprotein, cells were incubated for 1 hour at 4°C with 83A25 rat monoclonal antibody (a gift from Leonard Evans, National Institute of Allergy and Infectious Diseases, Hamilton, MT) *(29)*. The cells were washed twice with PBS with 1% (w/v) BSA then incubated with Alexa Fluor 647 goat anti-Rat IgG (Life Technologies) for 30 minutes. Then the cells were washed twice and either labeled with additional fluorochrome-conjugated mAb or analyzed. Staining of phospho-p65 and phospho-p105 was performed by first staining surface markers CD19, B220, and NP-PE. Cells were then permeablized with Cell Fixation/Permeabilization Kit (BD Pharmingen) according to the manufacturer's instructions. Then the cells were stained with phospho-p65 or phospho-p105 antibodies (Cell Signaling), washed with FACS buffer (PBS, 0.5-1% (w/v) BSA, 0.1% (v/v) sodium azide), and stained with FITC-anti-rabbit IgG (Jackson ImmunoResearch) for 30 min before two washes with FACS buffer. Data were acquired on an LSRFortessa cell analyzer (BD Bioscience) and analyzed with FlowJo software (Treestar). Sorting was performed on a FACSAria II cell sorter (BD Bioscience).

BrdU labeling

BrdU labeling and detection was performed with the APC BrdU Flow Kit (BD Bioscience) according to manufacturer's instructions.

Determination of cGAMP abundance using LC-MS/MS

Viable NP-specific and non-NP-specific splenic $CD19^+$ B cells from naïve or immunized mice were sorted into ice cold saline using a FACSAria II cell sorter. Cells were washed with ice cold saline, pelleted by centrifugation at 1000*g*, then suspended in 0.5 ml cold methanol/water (80/20, *v/v*). Cells were transferred to an eppendorf tube and subjected to three freeze-thaw cycles. After vigorous vortexing, the debris was pelleted by centrifugation at 16,000*g* at 4°C for 15 min. The supernatant was transferred to a new tube and evaporated to dryness using a SpeedVac concentrator (Thermo Savant, Holbrook, NY). Metabolites were reconstituted in 50 µl of 0.1% *v/v* formic acid in analytical-grade water, vortex-mixed and centrifuged to remove debris. Thereafter, the supernatant was transferred to a HPLC vial for the analysis of cGAMP.

Sample separation was achieved on a Phenomenex Synergi Polar-RP HPLC column (150 × 2 mm, 4 µm, 80 Å) using a Nexera Ultra High Performance Liquid Chromatograph (UHPLC) system (Shimadzu Corporation, Kyoto, Japan). The mobile phases employed were 0.1% *v/v* formic acid in water (A) and 0.1% *v/v* formic acid in acetonitrile (B). The gradient program was as follows: 0-0.5 min, 100% A; 0.5-5 min, 100% - 0% A; 5-6 min, 0% A; 6-6.1 min, 0% - 100% A; 6.1-10 min, 100% A. The column was maintained at 35°C and the samples kept in the autosampler at 4°C. The flow rate was 0.5 ml/min, and injection volume 10 µl. The mass spectrometer was an AB QTRAP 5500 (Applied Biosystems SCIEX, Foster City, CA) with electrospray ionization (ESI) source in multiple reaction monitoring (MRM) mode. Sample analysis was performed in positive mode. Declustering potential (DP) and collision energy (CE) were optimized by direct infusion of reference standards using syringe pump prior to sample analysis. The MRM MS/MS detector conditions were set as follows: curtain gas 30 psi; ion spray voltages 5000 V; temperature 650°C; ion source gas 1 50 psi; ion source gas 2 50 psi; interface heater on; entrance potential 10 V. In total, four ion pairs were monitored for the determination of cGAMP. The MRM transitions (*m/z*), DPs (V) and CEs (V) of the detected metabolites were 675 > 524, 60 V, 25 V; 675 > 136, 60 V, 41 V; 338 > 152, 60 V, 17 V; 338 > 136, 60 V, 23 V, respectively. Dwell time for each transition was set at 100 msec. Cell samples were analyzed in a randomized order, and MRM data was acquired using Analyst 1.6.1 software (Applied Biosystems SCIEX, Foster City, CA). Chromatograms of cGAMP shown in Fig. 2 were regenerated on the basis of the data exported from the raw chromatographic files using GraphPad for high-resolution purposes. Chromatogram review and peak area integration were performed using MultiQuant software version 2.1 (Applied Biosystems SCIEX, Foster City, CA). The peak area of the MRM transition 338 > 152, which provides the highest intensity, was selected for the analysis of cGAMP. Although the numbers of cells were very similar and each sample was processed identically and randomly, the peak area for each detected metabolite was normalized against the viable cell number of that sample to correct any variations introduced from sample handling through instrument analysis. The normalized area values were used as variables for statistical data analysis using Student's *t* test. P values < 0.05 were considered statistically significant.

B cell culture, transfection, and anti-IgM treatment

Mouse and human B cells were cultured in RPMI-1640 complete medium (RPMI-1640 medium supplemented with 10% *v/v* heat-inactivated FBS, 100 U/ml penicillin and streptomycin, 0.1 mM nonessential amino acids, 1 mM sodium pyruvate, and 0.1 mM β-mercaptoethanol (Life Technologies).

Splenic B cells ($CD19^+$) were isolated from naïve C57BL/6J mice using the Mouse Pan B Cell Isolation Kit (Miltenyi Biotec) and transfection of *pmaxGFP™ Vector* (Lonza) was performed using Nucleofector™ Kits for Stimulated Mouse B Cells (Lonza) according to the manufacturer's instructions without the activation step.

Mouse splenic B cells were negatively isolated using the Pan B Cell Isolation Kit (Miltenyi Biotec) and treated with either vehicle (PBS) or 130 μg/ml anti-IgM (Jackson ImmunoResearch).

The assay for nuclear translocation of p65 was performed using TransAM® NFκB p65 Kit (Active Motif) according to the manufacturer's instructions.

Human B cells were isolated using the Human B Cell Isolation Kit (Miltenyi Biotec). Human B cells were treated with vehicle (PBS), 1 mg/ml anti-IgM, or 1 mg/ml anti-IgM + 10 nM BTK inhibitor Ibrutinib (Selleckchem) for 2 days.

In vitro cGAMP and RT inhibitor treatment of B cells

Splenic B cells were negatively enriched using the Mouse Pan B-Cell Isolation Kit (Miltenyi Biotec). Human B cells were isolated using the Human B Cell Isolation Kit (Miltenyi Biotec). For *in vitro* cGAMP activation assay, 2×10^6 B cells were treated for 30 minutes at 37°C with either digitonin permeabilization solution alone (as the vehicle control) (50 mM HEPES pH 7.0, 100 mM KCl, 3 mM $MgCl_2$, 0.1 mM DTT, 85 mM Sucrose, 0.2% (w/v) BSA, 10 μg/mL Digitonin, 1 mM ATP, 0.1 mM GTP) or 2'3'-cGAMP standard (Invivogen) dissolved in digitonin permeabilization solution and added to cells at a final concentration of 30 μM *(30)*. Then the cells were washed twice with RPMI-1640 complete medium. After washing, 2'3'-cGAMP-treated cells were resuspended in RPMI-1640 complete medium with 0.6 μM 2'3'-cGAMP and control vehicle-treated cells were resuspended in RPMI-1640 complete medium and cultured for 2 days. Cells were subjected to flow cytometric analysis of surface activation markers on viable cells.

For *in vitro* RT inhibitor treatment, 2×10^6 B cells were treated with 200 μg NP_{49}-AECM-Ficoll, with 200 μg NP_{49}-AECM-Ficoll plus 10 μM each AZT, NVP, and ddI (Selleckchem) in RPMI-1640 complete medium, or with 1% (*v/v*) DMSO in RPMI-1640 complete medium (as the vehicle control) for 2 days. Viable B cells were analyzed for NP specificity and surface activation marker expression by flow cytometry.

Transfection of BMDMs and Q-PCR analysis

Bone marrow cells were collected from femurs and tibiae of mice. Cells were cultured in DMEM containing 10% FBS, antibiotics, and conditioned media from L929 cell culture. 24 hr later, non-adherent cells were transferred to a new plate and fresh conditioned media was added every other day up to the 7th day. Mature macrophages was harvested and transferred to new plates for further experiments.

Total RNA from viable NP-specific and non-NP-specific B cells was isolated as described below for RT-qPCR. Transfection of RNA into BMDM isolated from wild

type or mutant mice was carried out using Lipofectamine 2000 (Invitrogen). For enzyme treatments of nucleic acids, 1.0 μg of nucleic acids was treated with RNase V1 (Ambion) at 37°C for 1 hour before transfection. 7 hr after transfection, RNA was extracted from the transfected BMDM. To extract RNA, cells were first lysed in 1.0 ml of TRIzol (Invitrogen). Lysate was mixed with chloroform, and the aqueous phase was applied to RNeasy columns to obtain total RNA (Qiagen). The iScript cDNA synthesis kit (BioRad) was used to create cDNA from 0.15 mg of RNA. Quantitative real time PCR was performed in triplicate for each condition using Sybr Green on an Applied Biosystem Vii7 with the corresponding primers.

RNA immunoprecipitation-reverse transcription PCR (RIP-RT-PCR)

RNA bound to RIG-I was isolated with Magna RIP™ RNA-Binding Protein Immunoprecipitation Kit (Millipore) according to the manufacturer's instructions followed by RT-qPCR.

Quantitative RT-PCR and quantitative PCR

For RT-qPCR, RNA was isolated from viable NP-specific and non-NP-specific splenic $CD19^+$ sorted B cells using TRI reagent (Sigma-Aldrich) according to the manufacturer's instructions. DNase digestion and clean-up was performed with the Maxima First Strand cDNA Synthesis Kit for RT-qPCR (Thermo Scientific) and cDNA produced with SuperScript III First-Strand Synthesis System for RT-PCR (Life Technologies). For qPCR, the cytoplasmic material from viable NP-specific or non-NP-specific splenic $CD19^+$ sorted B cells was extracted using the RLN buffer (Qiagen) according to the instructions for RNeasy mini kit, and DNA from the cytoplasmic fraction was isolated using TRI reagent according to the manufacturer's instructions. RNase-free water (Qiagen) or nuclease-free water (Qiagen) was used throughout the procedures. Purified cDNA or cytoplasmic DNA was then used as the template for amplification of target gene transcripts using the StepOnePlus™ Real-Time PCR System (Life technologies) with iTaq™ Universal SYBR® Green Supermix (Bio-Rad Laboratories). Primer sequences are listed in Table S1.

RT activity assay

For RT activity in B cells, 3×10^5 viable NP-specific B cells from immunized C57BL/6J mice were sorted into ice cold saline using a FACSAria II cell sorter. Cells were washed with ice cold saline, pelleted by centrifugation at 1000*g*, then suspended and lysed with 20 μl 1% (*v/v*) Triton-X-100. The RT activity in the cell lysates was measured with the EnzChek® Reverse Transcriptase Assay Kit (Invitrogen) according to the manufacturer's instructions. For RT activity in the supernatants of B cells, 1×10^6 viable NP-specific or non-NP-specific $CD19^+$ B cells were sorted from immunized $Igh^{B1\text{-}8^+}$ transgenic mice on day 4 post-immunization and cultured in 100 μl of media alone, media containing 200 μg NP-Ficoll, or media containing 10 μg/ml ultrapure LPS (Invivogen). After 1.5 days, cells and culture media were centrifuged at 900*g* and the supernatants were harvested for measurement of RT activity with the EnzChek® Reverse Transcriptase Assay Kit according to the manufacturer's instructions.

Generation of $cGas^{-/-}$;$Mavs^{-/-}$ mice using the CRISPR system

Female *cGas*$^{-/-}$ mice were superovulated by injection with 6.5 U pregnant mare serum gonadotropin (PMSG; Millipore), then 6.5 U human chorionic gonadotropin (hCG; Sigma-Aldrich) 48 hours later. The superovulated mice were subsequently mated with *cGas*$^{-/-}$ male mice overnight. The following day, fertilized eggs were collected from the oviducts and *in vitro* transcribed Cas9 mRNA (50 ng/μl) and MAVS small base-paring guide RNA (50 ng/μl; 5′-ATCGACTGCGGGCTTCCTAC-3′) were injected into the cytoplasm or pronucleus of the embryos. The injected embryos were cultured in M16 medium (Sigma-Aldrich) at 37°C and 95% air/5% CO2. For the production of mutant mice, 2-cell stage embryos were transferred into the ampulla of the oviduct (10-20 embryos per oviduct) of pseudopregnant Hsd:ICR (CD-1) (Harlan Laboratories) females.

Immunofluorescence staining

Tissues were embedded in Tissue-Tek O.C.T. compound (Sakura), snap-frozen in liquid nitrogen, and stored at −80 °C. Cryostat sections 5 μm in thickness were mounted onto glass slides, air dried, and fixed in acetone at -20°C for 20 min, followed by two washes with washing buffer (PBS with 0.5% (v/v) Tween-20). Tissue sections were then blocked with SNIPER Blocking Reagent (Biocare Medical) for 30 min at room temperature. Primary antibodies Alexa Fluor 647-conjugated rat anti-mouse IgD (BioLegend), FITC-conjugated rat anti-mouse MOMA-1 (also called CD169) (AbD Serotec), or biotinylated rat anti-mouse DC-SIGNR1 (Acris Antibodies Inc.) were diluted in TNB (0.1 M Tris-HCl pH 7.5, 0.15 M NaCl, 0.05% (v/v) Tween-20) with 10% SNIPER Blocking Reagent (Biocare Medical) and sections incubated at room temperature for 120 min. After the primary antibody incubation, sections were washed with washing buffer and then either mounted using Aqua Poly/Mount (Polysciences, Inc.) (for IgD and MOMA-1 staining) or incubated with Alexa Fluor 488-conjugated streptavidin (Invitrogen) in TNB for 2 hr at room temperature (for IgD and DC-SIGR1 staining). Following incubation with secondary antibody, sections were washed with washing buffer and mounted using Aqua Poly/Mount (Polysciences Inc.).

Statistical analyses

Data represent means ± SEM in all graphs depicting error bars. The statistical significance of differences between experimental groups was determined using GraphPad Prism 6 and the indicated statistical tests. *P* values are indicated by * $P \leq 0.05$; ** $P \leq 0.01$; *** $P \leq 0.001$; **** $P \leq 0.0001$; ns, not significant with $P > 0.05$.

Supplementary Text

Normal development of MZ, B-1, and B-2 B cells in STING-, MAVS-, or cGAS-deficient mice

Since the TI humoral response is mediated largely by marginal zone (MZ) and B-1 B cells *(31)*, we evaluated those cell populations in STING-, cGAS-, and MAVS-deficient mice (fig. S2A). Frequencies and numbers of splenic MZ, B-1, B-1a, and B-1b B cells, and peritoneal cavity B-1, B-1a, and B1-b B cells, and other major lymphocyte populations were normal in each of the three mutant strains (fig. S2B-F). These data suggest a specific requirement, outside of MZ and B-1 B cell developmental pathways, for cytosolic DNA and RNA sensing in the TI-2 response to NP-Ficoll. In support of this

conclusion, we found that the frequencies of NP-specific MZ and B-1 B cells in STING-, cGAS-, and MAVS-deficient mice were significantly lower than in C57BL/6J mice following NP-Ficoll immunization (fig. S3).

Normal NP capture by MZ B cells and MZ macrophages

In the spleen, MZ B cells directly capture TI-2 antigens, or are exposed to them by metallophilic and MZ macrophages that also capture TI-2 antigens *(32)*. Thirty minutes following i.v. immunization with NP-Ficoll, we observed normal levels of NP binding by cGAS- and MAVS-deficient MZ B cells and MZ macrophages (fig. S4A and B). Both MZ and metallophilic macrophages were present with normal frequencies in cGAS- and MAVS-deficient spleens (fig. S4C), and showed a wild type staining pattern in spleen sections from STING-, cGAS-, and MAVS-deficient mice (fig. S4D and E). No gross morphological defects of MZ structure were observed in the mutant strains. Thus, defective TI-2 antibody responses of cGAS- and MAVS-deficient mice likely do not arise from impaired antigen capture in the MZ.

B cell activation by cGAMP

To determine whether cytosolic DNA can activate B cells *in vitro*, we transfected a green fluorescent protein (GFP)-encoding plasmid into mouse splenic B cells (fig. S6) and measured activation marker expression. GFP-expressing B cells from C57BL/6J mice upregulated activation marker expression 3- to 16-fold, and showed increased BrdU incorporation, relative to mock transfected cells, whereas no upregulation was observed in transfected GFP-negative cells (Fig. 2A). When B cells from STING-deficient mice were transfected with the same plasmid, they failed to become activated (Fig. 2A). Thus, the presence of DNA in the cytoplasm is sufficient to activate B cells, and appears to be sensed exclusively by the cGAS-STING pathway. In agreement, on day 4.5 after immunization of C57BL/6J mice with NP-Ficoll, cGAMP levels in NP-specific B cells, but not B cells with non-NP specificities, were elevated 8-fold relative to levels in naïve B cells (Fig. 2B). Examination of cGAMP levels over time revealed a persistent increase lasting for at least 10 days in NP-specific B cells (Fig. 2C). Thus, cGAMP is specifically elevated in activated antigen-specific B cells *in vivo*. Consistent with adoptive transfer experiments (Fig. 1D), these findings support a B cell-intrinsic function for cGAS-STING signaling in B cells activated by TI-2 antigens.

C57BL/6J B cells treated with cGAMP *in vitro* displayed increases in CD86 and BrdU uptake relative to control cells incubated with vehicle alone (Fig. 2D and E). cGAMP treatment also drove the activation of cGAS-deficient B cells *in vivo*, as shown by the partial rescue of NP-specific IgM levels in the serum of cGAS-deficient mice immunized with NP-Ficoll together with cGAMP (Fig. 2F). In contrast, CD86 expression and BrdU uptake by STING-deficient B cells treated with cGAMP was not significantly different from control cells incubated with vehicle alone (Fig. 2D and E). Thus, cGAMP is sufficient to drive mouse B cell activation, and does so in a STING-dependent manner. These findings are consistent with a previous report that cGAMP functions as an adjuvant to stimulate antibody production during TD immunization *(14)*.

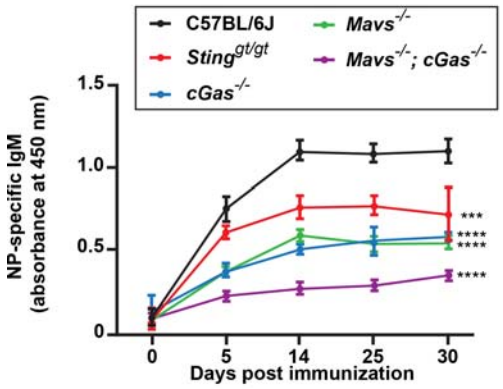

Fig. S1.

Timecourse of serum NP-specific IgM levels in mice immunized with NP-Ficoll. NP-specific IgM was measured by ELISA. *N* = 5 C57BL/6J mice, 5 *Sting*$^{gt/gt}$ mice, 5 *Mavs*$^{-/-}$ mice, 5 *cGas*$^{-/-}$ mice, 3 *cGas*$^{-/-}$;*Mavs*$^{-/-}$ mice. The significance of differences between each mutant genotype and C57BL/6J on day 30 is indicated; *P* values were determined by one-way ANOVA and post hoc Tukey test. Results are representative of 2 independent experiments.

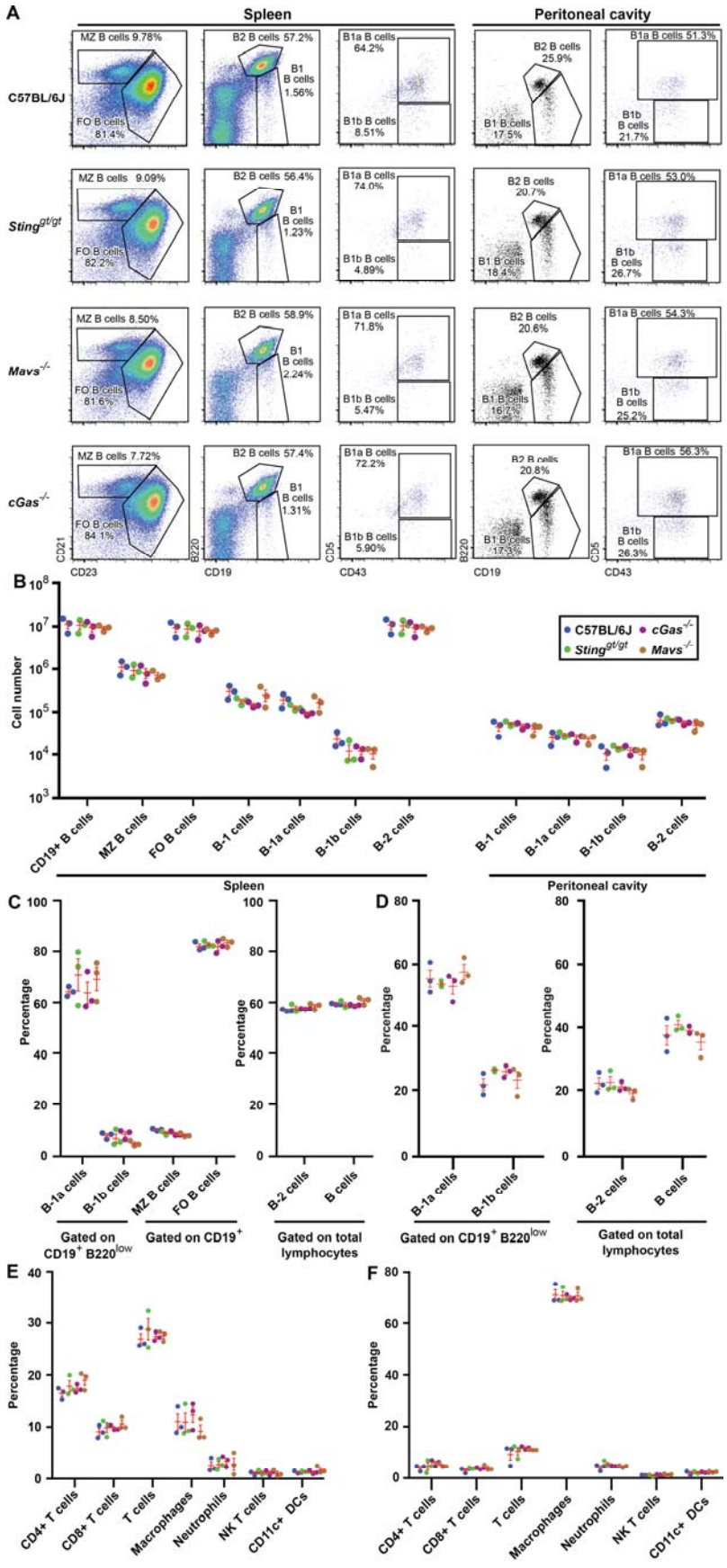
A
Spleen
Peritoneal cavity
C57BL/6J
Sting gt/gt
Mavs -/-
cGas -/-
MZ B cells 9.78%
FO B cells 81.4%
B2 B cells 57.2%
B1 B cells 1.56%
B1a B cells 64.2%
B1b B cells 8.51%
B2 B cells 25.9%
B1 B cells 17.5%
B1a B cells 51.3%
B1b B cells 21.7%
MZ B cells 9.09%
FO B cells 82.2%
B2 B cells 56.4%
B1 B cells 1.23%
B1a B cells 74.0%
B1b B cells 4.89%
B2 B cells 20.7%
B1 B cells 18.4%
B1a B cells 53.0%
B1b B cells 26.7%
MZ B cells 8.50%
FO B cells 81.6%
B2 B cells 58.9%
B1 B cells 2.24%
B1a B cells 71.8%
B1b B cells 5.47%
B2 B cells 20.6%
B1 B cells 16.2%
B1a B cells 54.3%
B1b B cells 25.2%
MZ B cells 7.72%
FO B cells 84.1%
B2 B cells 57.4%
B1 B cells 1.31%
B1a B cells 72.2%
B1b B cells 5.90%
B2 B cells 20.8%
B1 B cells 17.1%
B1a B cells 56.3%
B1b B cells 26.3%
CD21
CD23
B220
CD19
CD5
CD43
B
Cell number
C57BL/6J
cGas -/-
Sting gt/gt
Mavs -/-
CD19+ B cells
MZ B cells
FO B cells
B-1 cells
B-1a cells
B-1b cells
B-2 cells
Spleen
Peritoneal cavity
C
D
Percentage
Gated on CD19+ B220low
Gated on CD19+
Gated on total lymphocytes
E
F
CD4+ T cells
CD8+ T cells
T cells
Macrophages
Neutrophils
NK T cells
CD11c+ DCs

Fig. S2

Normal development of MZ, B-1, and B-2 B cells in STING-, MAVS-, or cGAS-deficient mice. (A) Representative flow cytometric analysis of MZ, B-1, B-1a, B-1b, and B-2 B cells in the spleen and peritoneal cavity using the following markers: marginal zone (MZ) B cells ($CD21^{high}CD23^{low}CD19^{+}$), follicular (FO) B cells ($CD21^{low}CD23^{high}CD19^{+}$), B-1 B cells ($CD19^{+}B220^{low}$), B-1a B cells ($CD5^{+}CD43^{+}CD19^{+}B220^{low}$), B-1b B cells ($CD5^{-}CD43^{+}CD19^{+}B220^{low}$), and B-2 B cells ($CD19^{+}B220^{high}$). The frequency of each cell type is indicated, with $CD21^{high}CD23^{low}$ MZ B cells shown as a percentage of $CD19^{+}$ cells; $CD21^{low}CD23^{high}$ FO B cells as a percentage of $CD19^{+}$ cells; $CD5^{+}CD43^{+}$ B-1a B cells as a percentage of $CD19^{+}B220^{low}$ cells; $CD5^{-}CD43^{+}$ B-1b B cells as a percentage of $CD19^{+}B220^{low}$ cells; $CD19^{+}B220^{low}$ B-1 B cells as a percentage of total lymphocytes; $CD19^{+}B220^{high}$ B-2 B cells as a percentage of total lymphocytes. (B) Numbers of B cells or cells of the indicated B cell subsets in the spleen or peritoneal cavity analyzed by flow cytometry as in (A). (C-F) Lymphocytes in the spleen (C and E) and peritoneal cavity (D and F) were analyzed by flow cytometry. (C and D) Frequencies of B cells and B cell subsets. $CD19^{+}$ B cells and $CD19^{+}B220^{high}$ B-2 B cells as a percentage of total lymphocytes; $CD5^{+}CD43^{+}$ B-1a B cells and $CD5^{-}CD43^{+}$ B-1b B cells as a percentage of $CD19^{+}B220^{low}$ cells; $CD21^{high}CD23^{low}$ MZ B cells and $CD21^{low}CD23^{high}$ FO B cells as a percentage of $CD19^{+}$ cells. (E and F) Frequencies of the indicated populations out of total lymphocytes. Data points represent individual mice. *P* values were determined by one-way ANOVA and post hoc Tukey test; in B-F, no significant difference was found between any mutant genotype and C57BL/6J. Data are representative of 2-3 independent experiments with at least 3 mice per group.

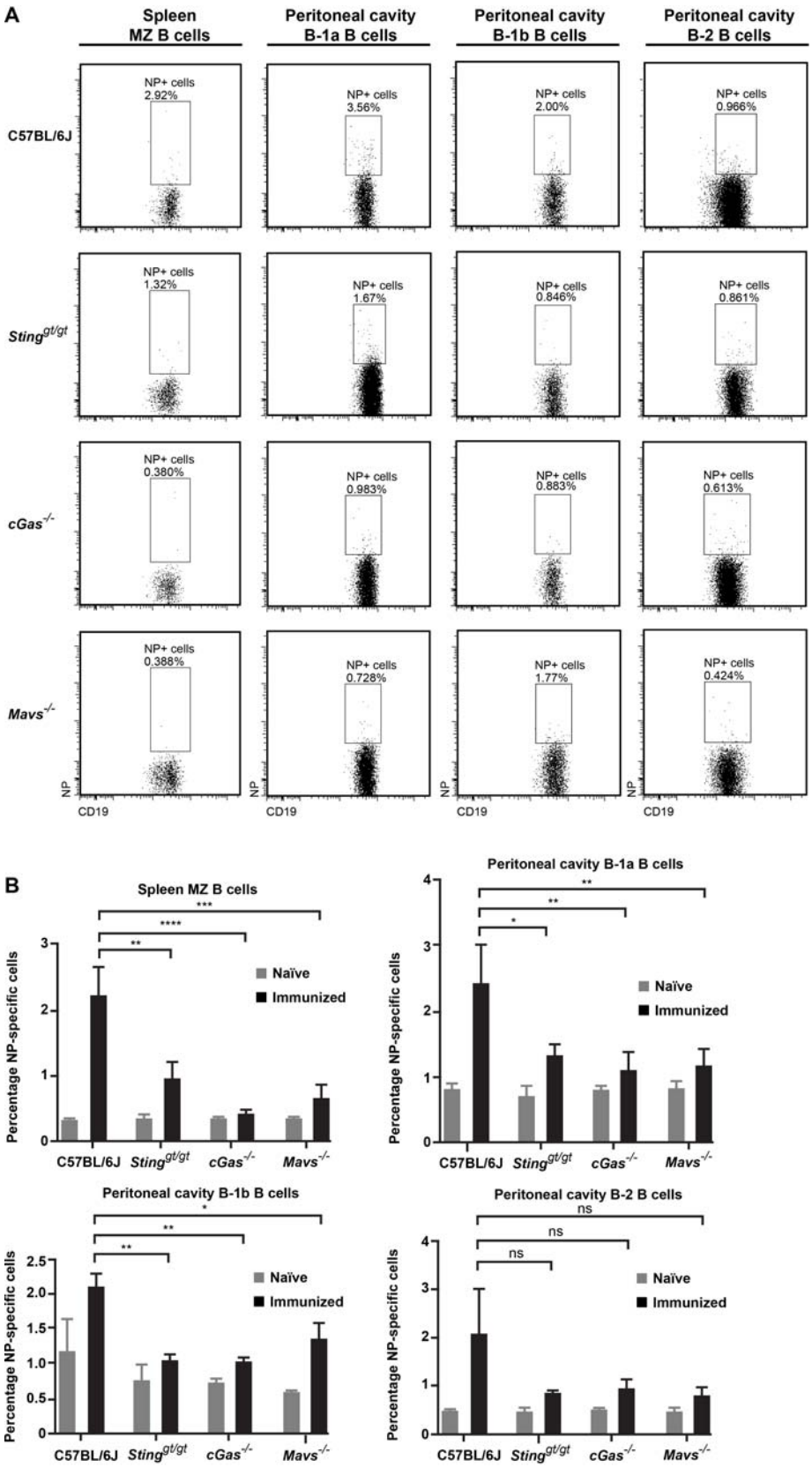
A
Spleen
MZ B cells
Peritoneal cavity
B-1a B cells
Peritoneal cavity
B-1b B cells
Peritoneal cavity
B-2 B cells
C57BL/6J
Sting gt/gt
cGas -/-
Mavs -/-
NP+ cells
2.92%
NP+ cells
3.56%
NP+ cells
2.00%
NP+ cells
0.966%
NP+ cells
1.32%
NP+ cells
1.67%
NP+ cells
0.846%
NP+ cells
0.861%
NP+ cells
0.380%
NP+ cells
0.983%
NP+ cells
0.883%
NP+ cells
0.613%
NP+ cells
0.388%
NP+ cells
0.728%
NP+ cells
1.77%
NP+ cells
0.424%
NP
CD19
B
Spleen MZ B cells
Peritoneal cavity B-1a B cells
Peritoneal cavity B-1b B cells
Peritoneal cavity B-2 B cells
Percentage NP-specific cells
Naïve
Immunized
C57BL/6J
Sting gt/gt
cGas -/-
Mavs -/-
ns

Fig. S3

Impaired upregulation of NP-specific MZ and B-1 B cells in STING-, MAVS-, or cGAS-deficient mice immunized with NP-Ficoll. (A) Representative flow cytometric analysis of NP-specific B cells on day 4.5 post-immunization. B cell subpopulations were first gated as in Fig. S2, then gated for $NP^{+}CD19^{+}$ cells. (B) NP-specific cells were analyzed on day 4.5 post-immunization or in naïve mice. NP-specific cells as a percentage of splenic $CD21^{high}CD23^{low}CD19^{+}$ MZ B cells (upper left), peritoneal cavity $CD5^{+}CD43^{+}CD19^{+}B220^{low}$ B-1a B cells (upper right), peritoneal cavity $CD5^{-}CD43^{+}CD19^{+}B220^{low}$ B-1b B cells (lower left), or peritoneal cavity $CD19^{+}B220^{high}$ B-2 B cells (lower right). N = 3 naïve, 3 immunized mice of each genotype. Results are representative of 2-3 independent experiments.

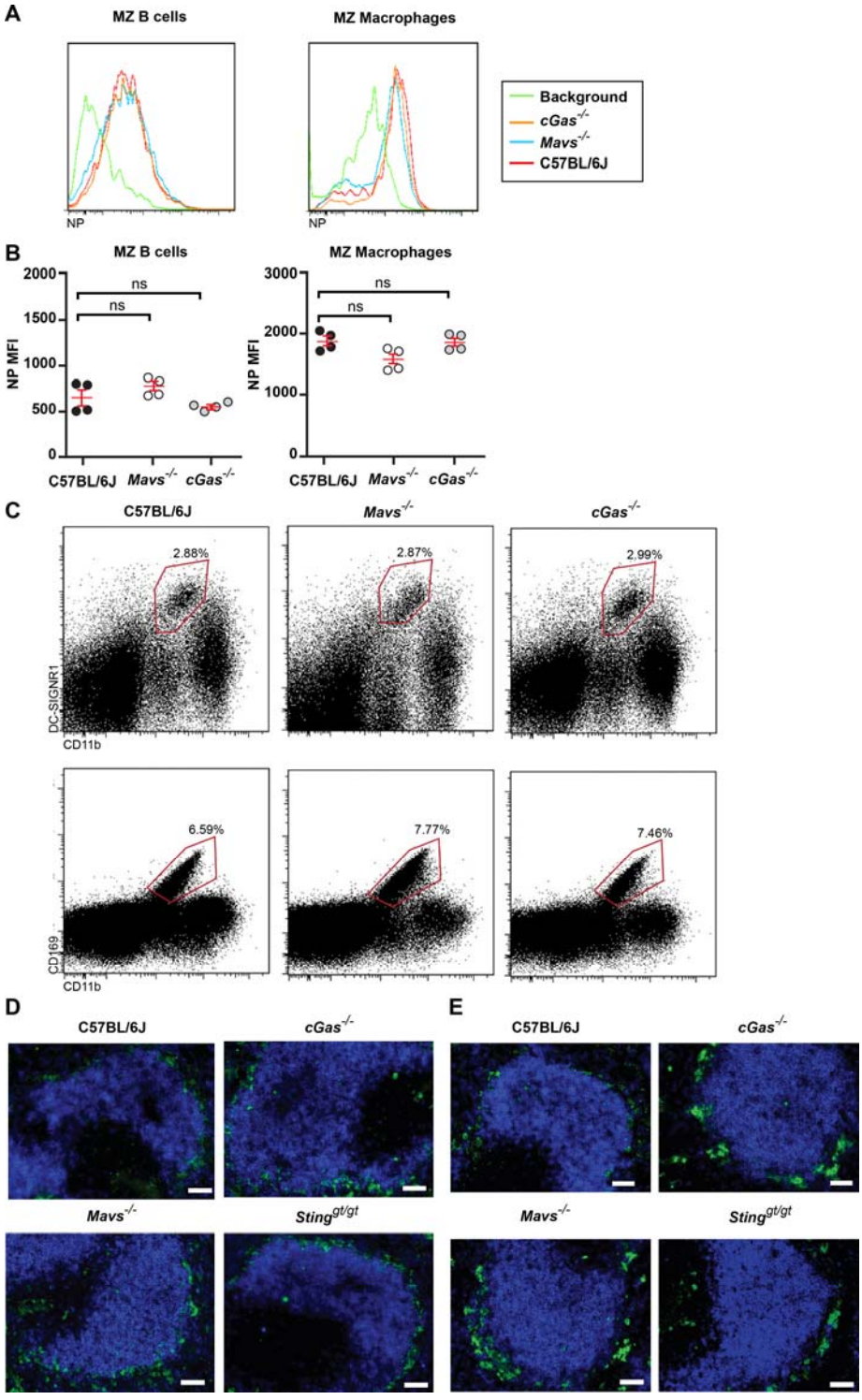

Fig. S4

Normal NP capture by MZ B cells and MZ macrophages. (A and B) Spleen cells were isolated from mice 30 min following i.v. immunization with NP-Ficoll, stained with anti-NP and cell-specific markers, and analyzed by flow cytometry. (A) Representative flow

cytometric analysis of NP captured by MZ B cells and MZ macrophages. Cells were gated using the following markers: MZ B cells ($CD19^+B220^+CD21^{high}CD23^{low}$) and MZ macrophages ($CD19^-CD11b^+$DC-$SIGNR1^+$). (B) NP capture by MZ B cells and MZ macrophages. MFI, mean fluorescence intensity. Data points represent individual mice. *P* values were determined by one-way ANOVA and post hoc Tukey test. (C) Representative flow cytometric analysis of splenic MZ macrophages ($CD11b^+$DC-$SIGNR1^+$) and metallophilic macrophages ($CD11b^+CD169^+$). Cells were first gated on the $CD19^-$ subpopulation. The frequencies of the gated subpopulations are indicated. (D and E) Splenic cryosections were stained with anti-IgD (blue) to label follicles. (D) Metallophilic macrophages were stained with anti-MOMA-1 (anti-CD169) (green). (E) MZ macrophages were stained with anti-DC-SIGNR1 (green). Scale bar, 50μm. Results are representative of 2 independent experiments.

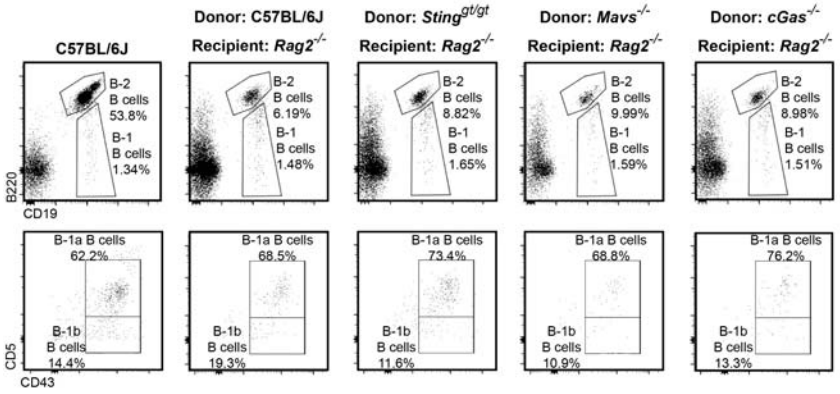

Fig. S5

Reconstitution of the B cell compartment by adoptive transfer. Splenic and peritoneal B cells isolated from mice of the indicated genotypes were transferred into *Rag2*$^{-/-}$ mice. Representative flow cytometric analysis of B cell subpopulations in the peripheral blood on day 1 post-transfer using the following markers: B-1 B cells (CD19^{+}B220^{low}), B-1a B cells (CD5^{+}CD43^{+}CD19^{+}B220^{low}), B-1b B cells (CD5^{-}CD43^{+}CD19^{+}B220^{low}), and B-2 B cells (CD19^{+}B220^{high}). The frequency of each cell type is indicated, with CD5^{+}CD43^{+} B-1a B cells as a percentage of CD19^{+}B220^{low} cells; CD5^{-}CD43^{+} B-1b B cells as a percentage of CD19^{+}B220^{low} cells; CD19^{+}B220^{low} B-1 B cells as a percentage of total lymphocytes; CD19^{+}B220^{high} B-2 B cells as a percentage of total lymphocytes. Results are representative of 2 independent experiments.

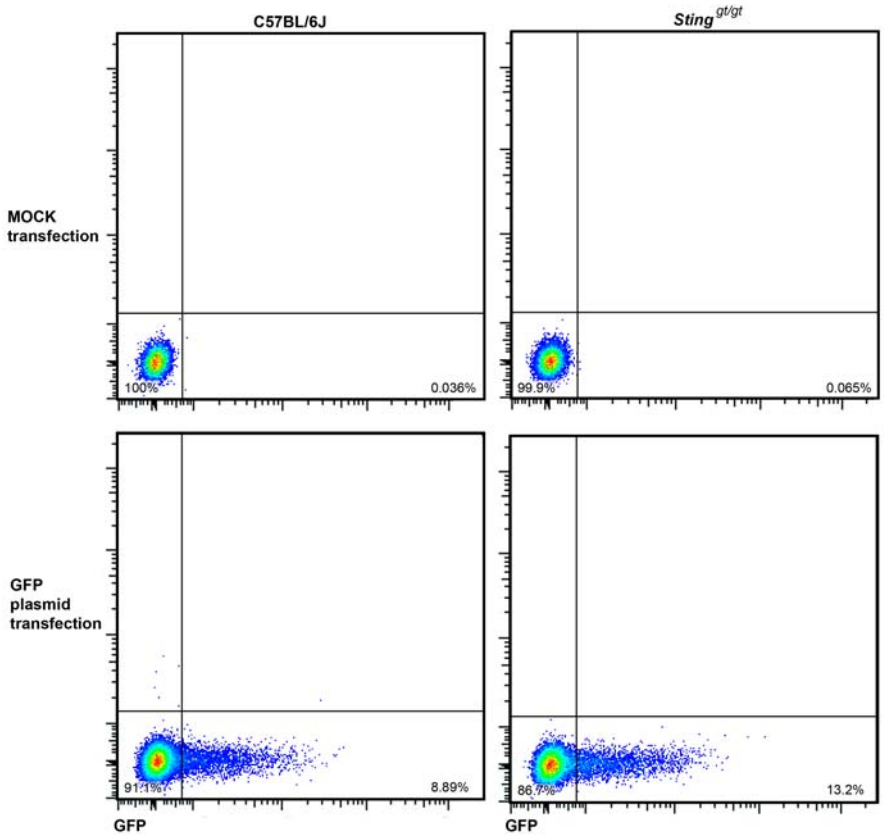

Fig. S6

GFP expression following transfection of B cells *in vitro*. Representative flow cytometric analysis of C57BL/6J or *Sting*$^{gt/gt}$ splenic CD19^{+} B cells cultured *in vitro* and transfected with a GFP-encoding plasmid. Percentages of gated populations are indicated. Results are representative of 2 independent experiments.

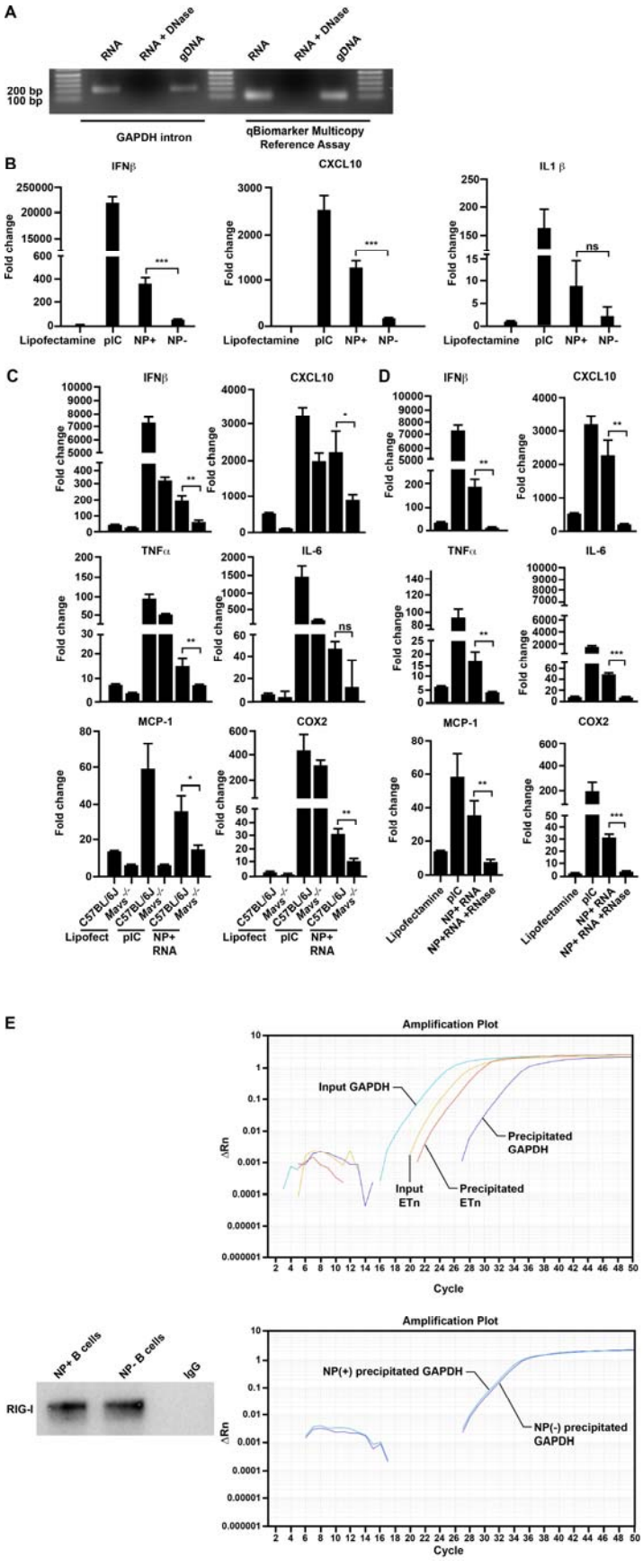
A
RNA
RNA + DNase
gDNA
RNA
RNA + DNase
gDNA
200 bp
100 bp
GAPDH intron
qBiomarker Multicopy Reference Assay
B
IFNβ
CXCL10
IL1 β
Fold change
Lipofectamine
pIC
NP+
NP-
ns
C
D
IFNβ
CXCL10
TNFα
IL-6
MCP-1
COX2
C57BL/6J
Mavs-/-
Lipofect
pIC
NP+ RNA
Lipofectamine
NP+ RNA +RNase
E
Amplification Plot
Input GAPDH
Precipitated GAPDH
Input ETn
Precipitated ETn
ΔRn
Cycle
NP+ B cells
NP- B cells
IgG
RIG-I
NP(+) precipitated GAPDH
NP(-) precipitated GAPDH

Fig. S7

Controls for measurements of ERV RNA. Splenic NP-specific or non-NP-specific $CD19^+$ B cells were collected by flow cytometry from C57BL/6J mice (A-D) or $Igh^{B1\text{-}8+}$ transgenic mice (E) 5 days post-immunization with NP-Ficoll. (A) RT-qPCR of mRNA isolated from NP-specific B cells ($N = 3$ mice) using primers specific for GAPDH or the Mouse Multicopy Reference PCR Assay, which targets a sequence present at more than 60 sites across the mouse genome. No DNA contamination was observed in the mRNA preparations, as shown by the absence of amplification products in reaction mixtures treated with DNAse according to the protocol used for all RT-PCR samples. This control may be most appropriate to exclude contamination by ERVs with similar or lower copy numbers in the genome, including endogenous MMTVs (~30 copies), xenotropic MLVs (~20 copies), polytropic MLVs (~40 copies), ecotropic MLVs (1 copy in C57BL/6J), MmERVs (~50 copies), and GLNs (~80 copies); DNA contamination by ERVs with higher copy numbers including IAPs (~1000 copies) cannot be definitively excluded. (B-D) Polyinosinic-polycytidylic acid (pIC) or pooled total RNA isolated from NP-specific or non-NP-specific B cells from 4 C57BL/6J mice was transfected into BMDM from C57BL/6J mice (B and D) or mice of the indicated genotypes (C). After 7 hr, expression of the indicated genes was measured by RT-qPCR of mRNA isolated from the BMDM. In D, NP-specific B cell RNA was treated with RNase prior to transfection as indicated. Results are representative of three independent experiments. (E) RT-qPCR amplification plot of ETn or GAPDH cDNA amplified from non-precipitated total mRNA (Input) or RIG-I-bound mRNA (Precipitated) isolated from NP-specific B cells (upper panel) ($N = 3$ mice). The specificity of the RIG-I interaction with ERV mRNA is supported by the observation that ~12.5% of total ETn mRNA was bound to RIG-I, while only 0.1% of total GAPDH mRNA was bound. The amount of immunoprecipitated RIG-I detected by RIG-I immunoblot (lower left panel) and GAPDH mRNA bound to RIG-I (lower right panel) was similar in NP-specific and non-NP-specific B cells.

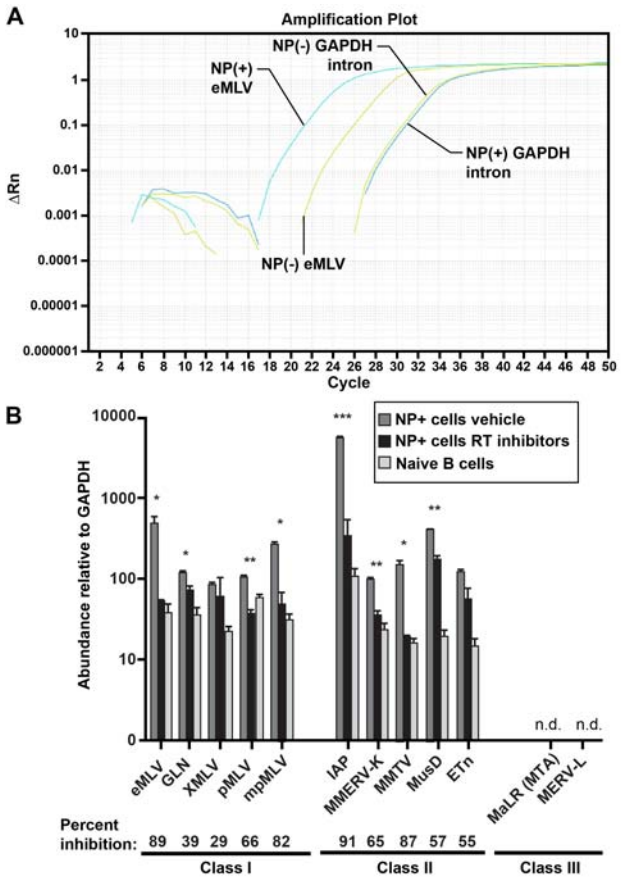

Fig. S8

Controls for measurements of ERV DNA in the cytoplasm. Splenic NP-specific or non-NP-specific CD19$^+$ B cells were collected by flow cytometry from C57BL/6J mice 5.5 days post-immunization with NP-Ficoll. (A) Examination of cytoplasmic DNA contamination by genomic DNA. qPCR amplification plot of eMLV or GAPDH intron DNA in the cytoplasmic fraction of NP-specific or non-NP-specific B cells (N = 3 mice). Cytoplasmic DNA samples from NP$^+$ and NP$^-$ cells contain similar low levels of genomic DNA, as measured by qPCR of a GAPDH intron sequence. Relative to GAPDH intron DNA, 40-fold and 5-fold higher levels of ERV DNA are present in NP$^+$ and NP$^-$ cells, respectively. (B) ERV DNA levels in the cytoplasmic fraction of naïve B cells, or NP-specific B cells from mice pretreated for 3 days with RT inhibitors (AZT, NVP) or vehicle and then immunized with NP-Ficoll (N = 3 mice per group). RT inhibitor treatment continued until day 4.5 post-immunization when B cells were collected. Percent reduction of ERV cDNA level in inhibitor-treated cells relative to vehicle-treated cells is indicated. Data were normalized to GAPDH intronic DNA levels in the same cells. P values were determined by one-way ANOVA and post hoc Tukey test. Asterisks represent the significance of differences between NP-specific B cells treated with vehicle vs. RT inhibitors. n.d., not detected.

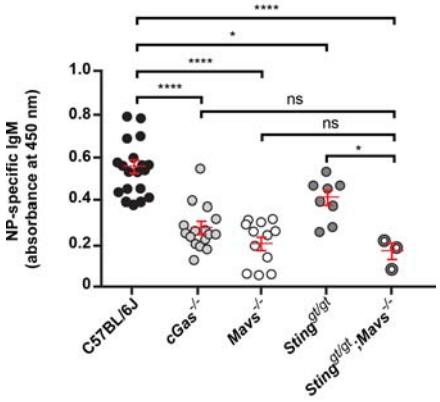

Fig. S9

Residual TI-2 antibody response in *Sting*$^{gt/gt}$;*Mavs*$^{-/-}$ mice. Serum NP-specific IgM on day 4.5 post-immunization with NP-Ficoll. Data points represent individual mice. *P* values were determined by one-way ANOVA and post hoc Tukey test. Results are representative of 2 independent experiments.

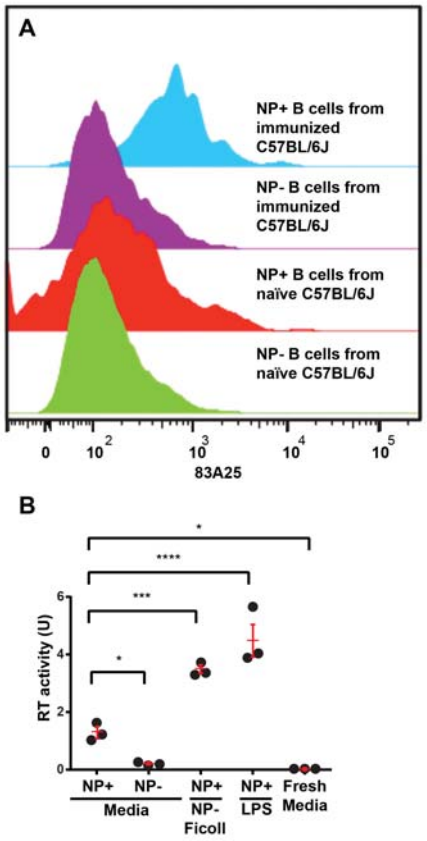

Fig. S10

Induction of ERV protein expression in NP-specific B cells from mice immunized with NP-Ficoll. NP-specific or non-NP-specific splenic CD19^{+} B cells were collected by flow cytometry from C57BL/6J (A) or *Igh*$^{B1\text{-}8+}$ transgenic mice (B) on day 4.5 post-immunization with NP-Ficoll. (A) Expression of endogenous MLV-specific Env glycoprotein assessed by 83A25 antibody staining and flow cytometry. Data are representative of 2 independent experiments with at least 3 mice per group. (B) NP-specific and non-NP-specific B cells were cultured *in vitro* for 1.5 days with media alone, media containing NP-Ficoll, or media containing LPS, and RT activity was measured in the culture supernatants. RT activity in fresh media without cells is also shown. Data points represent individual mice. *P* values were determined by one-way ANOVA and post hoc Tukey test.

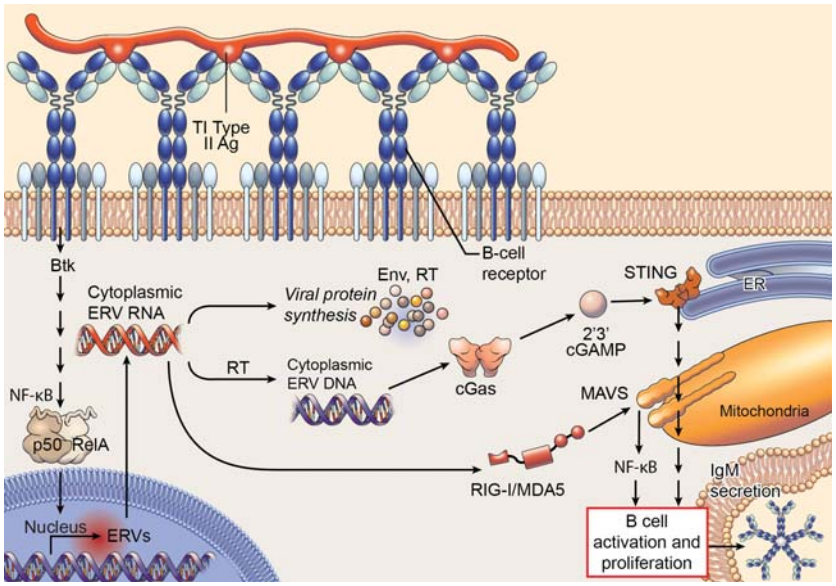

Fig. S11

Hypothetical model of signaling events in the TI-2 antibody response. Upon BCR engagement by TI-2 antigen, signaling from the BCR via Btk and NF-κB leads to transcriptional activation of numerous ERV genes. Resulting transcripts are translated to produce reverse transcriptase(s) (RT), endogenous MLV Env, and possibly other ERV proteins. The activity of RT enzymes results in retrotranscription of ERV mRNAs and consequent elevation of ERV cDNA in the cytoplasm of the same cell. These ERV mRNAs and cDNAs engage the RIG-I/MDA5-MAVS and the cGAS-STING pathways, respectively, to stimulate B cell activation and proliferation, and antigen-specific antibody production in a cell-intrinsic manner. Signaling from MAVS, but not cGAS-STING, activates NF-κB.

Table S1.

Primer Sequences

Oligo Name	Sequence 5' to 3'	Reference
eMLV spliced F	CCAGGGACCACCGACCCACCG	47
eMLV spliced R	TAGTCGGTCCCGGTAGGCCTCG	47
MMTV spliced F	AGAGCGGAACGGACTCACCA	47
MMTV spliced R	TCAGTGAAAGGTCGGATGAA	47
xMLV F	TCTATGGTACCTGGGGCTC	48
xMLV R	GGCAGAGGTATGGTTGGAGTAG	48
pMLV/mpMLV common F	CCGCCAGGTCCTCAATATAG	48
pMLV R	AGAAGGTGGGGCAGTCT	48
mpMLV R	CGTCCCAGGTTGATAGAGG	48
GLN F	TGTGTAAGTCCAGACGCAG	49
GLN R	CCAACCTACTCCAAAAACAG	49
IAP F	AAGCAGCAATCACCCACTTTGG	50
IAP R	CAATCATTAGATGCGGCTGCCAAG	50
MMERVK F	CAAATAGCCCTACCATATGTCAG	50
MMERVK R	GTATACTTTCTTCTTCAGGTCCAC	50
MaLR (MTA) F	ATGTTTTGGGGAGGACTGTG	50
MaLR (MTA) R	AGCCCCAGCTAACCAGAAC	50
MusD/EnTII common F	GTGCTAACCCAACGCTGGTTC	50
MusD R	CTCTGGCCTGAAACAACTCCTG	50
ETnII R	ACTGGGGCAATCCGCCTATTC	51
Mervl Pol F	ATCTCCTGGCACCTGGTATG	52
Mervl Pol R	AGAAGAAGGCATTTGCCAGA	52
Gapdh F	AGGCTCAAGGGCTTTTAAGG	
Gapdh R	ATCCTGTAGGCCAGGTGATG	
hLINE ORF1 F	TTGGAAAACACTCTGCAGGATATTAT	53
hLINE ORF1 R	TTGGCCTGCCTTGCTAGATT	53
HERV-W F	TGAGTCAATTCTCATACCTG	54
HERV-W R	AGTTAAGAGTTCTTGGGTGG	54
ERV F2B F	AAAAAGGAAGAAGTTAACAGC	54
ERV F2B R	ATATAAAGACTTAGGTCCTGC	54
HERV-E F	GGTGTCACTACTCAATACAC	54
HERV-E R	GCAGCCTAGGTCTCTGG	54
HERV F F	CCTCCAGTCACAACAACTC	54
HERV F R	TATTGAAGAAGGCGGCTGG	54
HERV-K(HML-2) F	AAAGAACCAGCCACCAGG	54
HERV-K(HML-2) R	CAGTCTGAAAACTTTTCTCTC	54
HERV-K(HML-5) F	TGAAAGGCCAGCTTGCTG	54
HERV-K(HML-5) R	CAATTAGGAAATTCTTTTCTAC	54

hGAPDH F	AGTCAACGGATTTGGTCGTATTGGG	54
hGAPDH R	ACGTACTCAGCGCCAGCATCG	54
IFN-β F	TCCGAGCAGAGATCTTCAGGAA	
IFN-β R	TGCAACCACCACTCATTCTGAG	
CXCL10 F	GCCGTCATTTTCTGCCTCA	
CXCL10 R	CGTCCTTGCGAGAGGGATC	
IL-6 F	TCCATCCAGTTGCCTTCTTG	
IL-6 R	GGTCTGTTGGGAGTGGTATC	
TNF-α F	CCTCCCTCTCATCAGTTCTATGG	
TNF-α R	GGCTACAGGCTTGTCACTCG	
COX-2 F	TCCTCACATCCCTGAGAACC	
COX-2 R	AAGTGGTAACCGCTCAGGTG	
MCP-1 F	AGGTCCCTGTCATGCTTCTG	
MCP-1 R	TGGGATCATCTTGCTGGTG	
GAPDH intron2 specific primers		http://www.cellsignal.com/products/chip-kits Reagents/8986?Ntt=GAPDH+Intron&fromPage=search
Multicopy Reference Assay		http://www.sabiosciences.com/preparecart.php?pcatn=VPM000-0000000A